Numerical study for the improvement of performance of Savonius wind turbine having elliptical blades

Pinku Debnath[1*], and *Ronald Debbarma*[2]

[1]Assistant Professor, Department of Mechanical Engineering, National Institute of Technology Agartala, Tripura, Jirania, India:799046
[2]B. Tech Student, Department of Mechanical Engineering, National Institute of Technology Agartala, Tripura, Jirania, India: 799046

Abstract. The S-rotor wind turbine operates based on drag, resulting in lower power coefficients. Furthermore, a multitude of geometric and aerodynamic factors have been meticulously crafted to enhance the overall efficiency. The augmentation technique decreased the adverse drag force produced by the S-rotor. Therefore, in this investigation, the elliptical bladed profile has been selected for simulation in conjunction with the curtain plate preceding the rotor. The simulation has been conducted in Ansys fluent platform. So far the comparison has been performed for power vs RPM for S-rotor blades and elliptical rotor blades. For elliptical rotor blades, the peak power magnitude of 10 W and average power of 7 W are achieved. From conventional S-rotor blades, the peak power magnitude of 8 W and average power of 4 W are obtained. It has been determined through contour plot analysis that the aerodynamic performance of an elliptical bladed profile with curtain plates surpasses that of an elliptical profile without curtains.

Keywords— Savonius wind turbine, Power output, Torque output, CFD, Elliptic blades.

1 Introduction

In the contemporary era, energy consumption has increased due to increase in world population. The availability of fossil energy sources is dwindling rapidly, leading to a shortage of these resources. Given the detrimental effects of fossil fuel energy sources on the environment, it is imperative to discover a clean and sustainable alternative energy source. Therefore, wind energy is an important source of free and green energy. The wind rotors are device for harnessing energy from wind. One such type of wind rotor is Savonius wind turbine. The performance of this type of rotor is lower but it has a number of advantages in comparison to conventional horizontal axis wind turbines [1, 2, 3]. The vertical-axis wind rotor known as the Savonius wind rotor was created by Finnish engineer Savonius SJ in 1925. The design of Savonius wind rotors is comparatively simple and cheap. Additionally, they begin to operate autonomously, regardless of the wind's direction.

* Corresponding author:er.pinkunits@yahoo.com

Additionally, they possess a significant initial torque. Despite the significant benefits they offer, Savonius wind turbines are not widely favored due to their limited aerodynamic efficiency. The current research project involved the development of a curtain aimed at enhancing the efficiency of the Savonius wind rotor. The numerical analysis of this curtain's impact on the rotor has been conducted [5, 6, 7]. Furthermore, an analysis was conducted on the pressure distributions surrounding the blades of the Savonius rotor in order to identify the regions of low and high pressure. These regions play a significant role in the overall generation of torque by the Savonius turbine. The experimental performance of the modified blade has been conducted to enhance the power coefficient of the Savonius rotor wind turbine [8, 9]. Wind tunnel tests have been conducted to investigate the impact of both single and multiple stages on power coefficient. Enhancing the quantity of stages decreases torque variations and is crucial for optimizing rotor efficiency. An experimental investigation was conducted to analyze the influence of Reynolds number, height to diameter ratio (h/d), and overlap ratio on the performance of Savonius rotor, revealing a beneficial effect on the power coefficient. The research focused on helical-shaped rotors revealed a higher power coefficient in comparison to the traditional semi-circular rotor design. Hence, modifications implemented in various parameters including the number of rotor stages, aspect ratio, overlap ratio, number of buckets, blade shape, and flow guide have been observed to greatly enhance the aerodynamic efficiency of the Savonius rotor [10, 11]. The experimental study conducted by Bhaumik T., et al. [12] aimed to determine the power coefficient of a two-bladed helical Savonius wind rotor at the exit of a centrifugal blower using five distinct overlap ratios. It was noted from their experimental analysis that Cp rises as the overlap ratio increases until a specific threshold, beyond which it continues to increase. Hence, there exists an optimal overlap ratio at which Cp reaches its maximum value. An optimal overlap ratio of 0.147 results in achieving the maximum Cp value of 0.421. Each blade was crafted with a twist angle of 45 degrees. Aluminum is utilized for the blade material of the rotor. Altan B. D., et al. [13] conducted research on enhancing the efficiency of Savonius wind rotors through the implementation of a modified curtain. The study focused on implementing a curtain design to enhance the efficiency of the Savonius wind rotor by mitigating the adverse effects of negative torque on the convex blade. The curtain has been positioned in front of the rotor, and performance tests have been conducted with and without the curtain in place. Kamoji M. A., et al. [14] conducted an experimental investigation on a modified Savonius rotor in a single stage. The study has concentrated on analyzing both traditional Savonius rotors and adapted Savonius rotors in order to enhance the power coefficient and achieve a consistent static torque coefficient. Additionally, the rotors are currently under investigation both with and without a central shaft positioned between the end plates. The experimental study was conducted in a closed jet wind tunnel on a modified version of the traditional Savonius rotor, which featured a central shaft and lacked a central shaft between the two end plates. The coefficient of power for a Savonius rotor with a central shaft is reportedly 0.32. A numerical analysis is conducted to examine how the performance of the rotors is influenced by various geometrical parameters, specifically in terms of the coefficient of static torque, coefficient of torque, and coefficient of power. The Savonius rotor with a modified design, featuring a blade arc angle of 124˚ and an aspect ratio of 0.7, achieves a maximum coefficient of power of 0.21 at Re=150000. This value surpasses the power coefficient of 0.19 exhibited by the conventional Savonius rotor. The research conducted by Mohamed M. H., et al. [15] focused on optimizing parameters of Savonius turbines by implementing an obstacle to shield the returning blade. An obstacle plate is implemented to partially shield the returning blade of a Savonius turbine, utilizing either two or three blades, in order to enhance wind direction towards the advancing blade. The torque coefficient is found to be even higher for larger values of the Tip speed ratio, as they have observed. Hence, the obstacle has a highly beneficial impact

on both designs. The two-blade configuration is evidently superior to the three-blade turbine due to the obtained output power coefficient, as well as the cost and complexity of the rotor. The peak power output coefficient reaches 0.258 with this ideal configuration at λ=0.8. It is evident from literature that CFD has the potential to serve as a valuable tool for analyzing the wind flow patterns around a helical Savonius rotor. According to the research conducted by Debnath P., et al. [16], it was discovered that a two-bladed rotor is more efficient when compared to a three-bladed rotor. Additionally, the study also observed that the helical Savonius rotor exhibits a positive torque coefficient at all rotor angles. The power coefficient of a modified Savonius wind rotor was investigated by Le A. D., et al. [17]. The enhanced rotor provides exceptional performance with a tip speed ratio (TSR) above 0.8. The wind turbine in urban areas typically operates at a TSR of 1.4, which is when it reaches its maximum power coefficient Cp. Numerical investigations were conducted by Alom N. et al. [18] on a rotor with elliptical blades augmented with vents. The simulation demonstrates a peak power coefficient (Cp) of 0.132 occurring at TSR=0.49. The numerical simulation for the modified rotor was conducted by Ramarajan J. and his colleagues [19] using the SST K-ω turbulence model. The modified blade has shown an increase in the power coefficient by Cp=0.2 when compared to the conventional blade shape. Kacprzak K, et al. [20] conducted research on Bach-type Savonius rotor. Their analysis demonstrated that within the tip speed ratio range of 0.2 to 0.4, the elliptical Savonius rotor outperforms the Bach-type Savonius rotor. Tartuferi M., et al. [21] studied on savonius rotor to enhance the aerodynamic performance of the wind rotor following the development of innovative air foil shaped blades namedSR3345 and SR5050 rotor and the use of a new curtain system, which is self-orienting relative to the wind flow direction. They found that curtain can enhance the performance. But orientation of curtain arrangement and Savonius blade shape is still in debate.

Best of the author's knowledge there are less information about power output from elliptical shape savonius wind rotor. The aim of this present numerical study to evaluate the comparison of power output from savonius wind turbine by using various blade profile at low wind speed regime.

2 Materials and methodology

2.1 Geometry of elliptical blade profile

The physical model of elliptical shape blades are depicted in Fig. 1.The elliptical rotor have been modelled using dimensions of OM/OC=2/3. The diameter measures 0.21 m, while the overlap ratio stands at 0.15. BB' represents the length of the cord of the rotor blade. The elliptical profile's sectional cut angle (θ) is considered to be 47.5˚. The rotor parameter aims to enhance blade performance by minimizing the counteracting torque that opposes the rotational momentum of the blades. In this scenario, a curtain plate has been analyzed for the purpose of eliminating the reverse direction moment. The geometric parameters were extracted from the experimental research carried out by Altan B. D., et al. [8]. The ratios of L1 to D and L2 to D are 2.14 and 2.48, respectively. The curtain has been positioned at an inclination of γ=15˚ and β=45˚ in front of the rotor blades. The curtain minimizes the adverse torque produced, enabling optimal utilization of the wind stream to impact the elliptical profile.

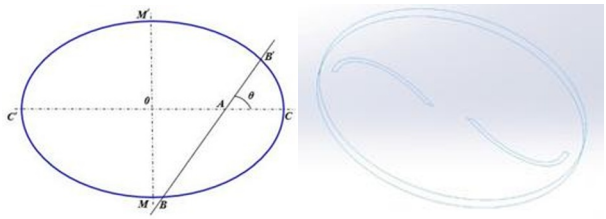

(a) (b)

Fig. 1. (a) The basic information of ellipse rotor from literature and (b) physical model design of elliptical profile Savonius blade.

2.2 Savonius rotor with curtain arrangement

The Fig. 2 shows the side and top view of elliptical Savonius rotor with curtain arrangement [18]. The Savonius wind rotor experiences a positive torque in the inner section of the cylinder, while a negative torque is generated in the outer section when the wind strikes it at a specific velocity. Due to the higher torque in the inner part compared to the outer part, the rotational movement occurs in a clockwise direction. The Savonius wind rotor's geometry was determined using a 2 mm thick steel sheet. The rotor has a diameter of 32 cm (D), a height of 32 cm (H), and an overlap ratio of 2.6 cm (e). The lower and upper end plates of the object have been constructed using a 4 mm thick steel sheet, which has a diameter of 35.2 cm. Figure 3 displays the physical representation of the Savonius wind rotor model. The Savonius wind rotor's shaft has been equipped with low friction ball bearings at both the top and bottom to reduce the friction force. The torque on the convex blade of the Savonius wind rotor appears to be lower than the torque on the concave blade due to the varying resistance coefficients of the surfaces. Due to this rationale, the Savonius wind rotor spins in the direction of the favorable torque that develops on the concave blade. In order to enhance the performance of the rotor, it is crucial to avoid the development of negative torque in the opposite direction of the rotor's rotation. A new design has been put forwarded to increase the performance of the Savonius rotor.

The Table 1 represents the details dimensions of curtain arrangement. In order to enhance the performance coefficients and harness the benefits of wind speed, a curtain configuration has been implemented in front of the rotor. In order to counteract the negative torque caused by the rotor's adverse rotating direction, this particular arrangement ensures that the angles of the curtain plates, denoted as α and β, as well as the lengths of the curtain plates, represented by L_1 and L_2, are carefully adjusted. The various curtain arrangements include curtain 1, curtain 2, and curtain 3, which are referred to as long, medium, and short curtains, respectively. The curtain arrangement consists of steel sheets that are 32 cm in height and 2 mm in thickness. The curtain's top and bottom sheets are secured, whereas the side sheets are crafted to be adjustable to accommodate any desired angle. The curtain arrangements have been designed in such a way that it can be rotates by 360˚ with ability to take in wind from all directions.

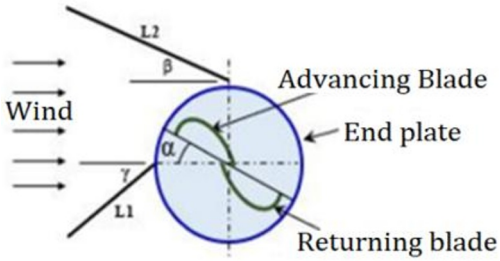

Fig. 2. Schematic view of Savonius rotor with curtain arrangement cited from literature.

Table 1. Dimensions of the curtain arrangement

Type of Curtain Arrangement	Length L_1 (cm)	Length L_2 (cm)	Height H (cm)	Thickness t (mm)
Curtain 1	45	52	32	2
Curtain 2	34	39	32	2
Curtain 3	22	26	32	2

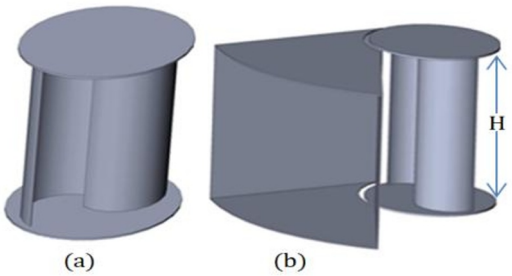

Fig. 3. The Savonius wind rotor (a) without and (b) with curtain arrangement.

2.3 Computational domain with rotor

The Fig. 4 shows the two dimensional sectional view of elliptic shape rotor with curtain arrangement in computational domain. The symmetry boundary conditions are specified at the top and bottom of the domain. The inlet is characterized by an incoming free-stream wind velocity. The curtain and rotor wall are regarded as conditions that do not allow slipping. The top and bottom wall are considered as symmetry. The wind velocity inlet and pressure outlet are present in computational domain.

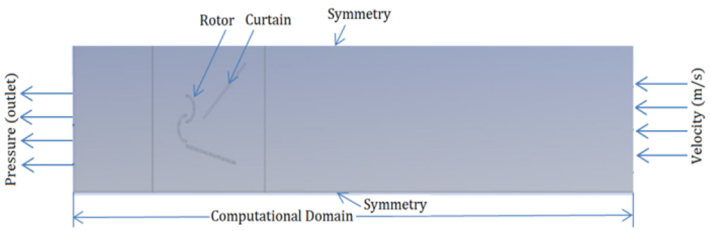

Fig. 4. Schematic appearance of the rotor arrangement with curtains in 2-D.

3 Governing equations

The mass, momentum and energy transports can represent by different differential equation. The conservative form of governing equations is given below:
Continuity equation:

$$\nabla.(\rho\vec{v})=0 \tag{1}$$

Momentum equation:

$$\frac{\partial}{\partial t}(\rho\vec{v}) + \nabla.(\rho\vec{v}\vec{v}) = -\nabla p + \rho\vec{g} + (\bar{\tau}) \tag{2}$$

Where, , $\bar{\tau}$ is the stress tensor,'p' is the static pressure, and $\rho\vec{g}$ is the gravity force. Assuming the Stokes's hypothesis for Newtonian fluid, the stress tensor $\bar{\tau}$ is given by

$$\bar{\tau} = \mu\left[\nabla.\vec{v} + \nabla.\vec{v}^{T} - {}^{2}/_{3}\,\nabla.\vec{v}I\right] \tag{3}$$

Furthermore, the turbulence closure model employed in this study is the standard k-**ϵ** model with standard wall condition. This model not only considers the conservative form of mass and momentum, but also solves a separate transport equation to independently determine the turbulence kinetic energy (k) and dissipation rate (**ϵ**). The model demonstrates high speed and performs effectively for flow with recirculation, which is why it is being utilized in the current research.:

$$\frac{\partial}{\partial t}(\rho k) + \frac{\partial}{\partial x_i}(\rho k u_i) = \frac{\partial}{\partial x_j}\left(\mu + \frac{\mu_t}{\sigma_k}\right)\frac{\partial k}{\partial x_j} + G_k - \rho\epsilon \tag{4}$$

$$\frac{\partial}{\partial t}(\rho\epsilon) + \frac{\partial}{\partial x_i}(\rho\epsilon u_i) = \frac{\partial}{\partial x_j}\left(\mu + \frac{\mu_t}{\sigma_\epsilon}\right)\frac{\partial \varepsilon}{\partial x_j} + C_{1\epsilon}\frac{\epsilon}{k}(G_k) - C_{2\epsilon}\rho\frac{\epsilon^2}{k} \tag{5}$$

Where, turbulent viscosity (μ_t) is given by:

$$\mu_t = \rho C_\mu \frac{k^2}{\epsilon}$$

In the above equations, G_k represents the generation of turbulence kinetic energy due to the mean velocity gradients. The C_μ, $C_{1\epsilon}$ and $C_{2\epsilon}$ are constants $\sigma_{\mathbf{k}}$ and $\sigma_{\boldsymbol{\epsilon}}$ are the turbulent Prandtl's number for turbulent kinetic energy (k) and energy dissipation rate (**ϵ**) respectively. After getting the velocity magnitude, the power is calculated by using the following formula:

$$P = \iiint_v \mu_1 \phi_v dv \tag{6}$$

Where, $\phi_v = 2\left[\left(\frac{dv_x}{dx}\right)^2 + \left(\frac{dv_y}{dy}\right)^2 + \left(\frac{dv_z}{dz}\right)^2\right] + \left[\frac{dv_x}{dy} + \frac{dv_y}{dx}\right]^2 + \left[\frac{dv_x}{dz} + \frac{dv_z}{dx}\right]^2 + \left[\frac{dv_y}{dz} + \frac{dv_x}{dy}\right]^2$
$\mu_1$is the apparent fluid viscosity.

$$P = 2\boldsymbol{\pi} N_s T_y + 2\boldsymbol{\pi} N_G T_z \tag{7}$$

Where, T_y and T_z are the torque near blade wall in y axis and z-axis respectively.
Also we can get torque by using Power, P=T×ω,where P is power, T is torque and ω is angular velocity.

4 Mesh generation and grid independency test

The Fig. 5 shows mesh structure near blade and computational domain. The inflation mesh has been used near the rotor. The fine mesh has been generated to the entire computational domain. The stationary area consists of a quadrilateral network. The rotating sector and the area upstream consist of quadrilateral components, which exhibit superior adaptability to intricate geometries. The mesh configuration surrounding the wind turbine rotor and the curtain has been enhanced in order to enhance the precision of the numerical modeling. Furthermore, a boundary layer containing five tiers of quadrangular cells is applied to the wind rotor blade in order to maintain a y+ value of less than 1, as mandated by the

turbulence model. The face sizing is also done in order to reduce the number of elements on remaining faces.

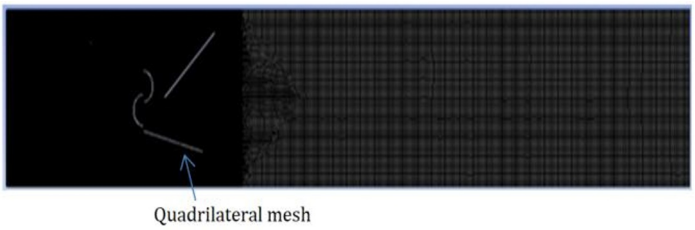

Fig. 5. Quadrilateral type mesh near the rotors with curtains in computational domain.

5 Numerical solver with boundary conditions

The CFD platform based on Fluent is utilized for evaluating the rotor's performance. The initial velocity magnitude of 7 m/s has been taken for the entire simulations. The conservative equations are solved through numerical simulations using the SIMPLE algorithm on an unstructured grid with the finite volume method. The rotor shifts its orientation from wind coming from upstream to wind coming from downstream. The rotor is set to rotate in 15˚ incrementsThe second order upwind discretization scheme was employed to ensure accuracy in the conservative terms of the momentum equation and turbulence equations. The Reynolds numbers are considered in laminar flow regimes.

6 Result and discussions

6.1 Power output analysis

The Fig. 6 shows the torque vs. RPM of Savonius wind rotor with curtain arrangement. The static torque values for curtain 1, curtain 2, curtain 3, and curtain less were analyzed numerically to determine the angle-related changes. This analysis was conducted for angles ranging from 30˚ to 90˚, with the rotor position set at 45˚ and β=45˚ and γ =15˚. The analysis was performed at various RPMs of the rotor. The torque values for curtain 1, the longest curtain, are observed to be greater than those for curtain 2 and curtain 3. The static torque values derived from numerical analysis at rotor positions of 45˚, 60˚, and 90˚. The numerical analysis indicates that the static torque values are highest at 45˚. In the current investigation, a curtain has been positioned in front of the rotor to enhance the rotational speed of Savonius wind rotors. In addition to controlling the angular velocity, measures must be taken to avoid the negative torque that impacts the convex surface of the wind rotor. The objective is to enhance the performance by increasing the velocity of the wind as it enters the rotational domain. The curtain angles (γ and β) are also placed for maximum output from the simulation. The negative torque rises as the flow encounters the convex blade at curtain angles less than 30˚ (γ<30˚), while the torque values obtained tend to decrease as the flow separations increase at curtain angles greater than 30˚ (β>30˚).

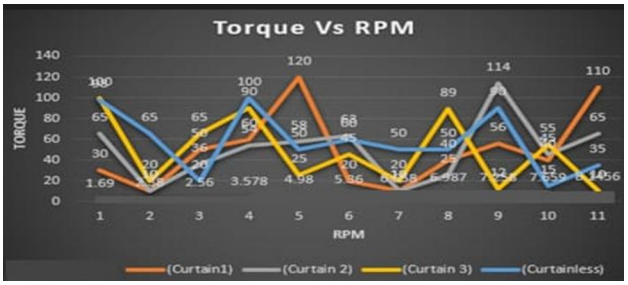

Fig. 6. Comparison of the torque changes with the rotor without curtain and the rotor with different curtain types for β=45˚ and γ=15˚.

6.2 Torque output analysis

The Fig. 7shows the power vs. RPM of Savonius wind rotor with curtain arrangement. It has been found that elliptical rotor blade gives better power output than S-rotor blade. When the rotor position is 45˚, 60˚ and 90˚ in the static position of the Savonius wind rotor having elliptical blades. The power outputs for curtains 1, 2, and 3 are determined by the rotor angle, which ranges from 30˚ to 60˚ during numerical analysis. This occurs when the rotor position is at 60˚, with γ=10˚ and β=15˚. The power values for curtain 1 are observed to be greater than those of curtain 2, curtain 3, and curtain less. The maximum torque value for curtain 1 was determined to occur at β=45˚ when γ=15˚. The numerical analysis yielded power values for curtain 1, curtain 2, and curtain 3 within the range of 30˚ to 60˚. These values were obtained with the rotor position set at 90˚, γ at 10˚, and β at 15˚. The rotor was subjected to numerical analysis with curtains of three different dimensions, and the highest power values were achieved with curtain Hence, numerical analysis has yielded the velocity distributions at which maximum power is achieved for rotor angles of 45˚, 60˚, and 90˚. When the rotor is positioned at 90˚, a significant portion of the fluid, which is directed by the curtain, exits over the convex blade, resulting in the generation of an unfavorable torque effect. The lowest torque values have been obtained at 90˚. Moreover, a greater amount of fluid seeps out from the space between the curtain end and rotor blade, consequently resulting in a reduction in the torque output value. At a rotor position of 45˚, an increased amount of fluid leaks out from between the curtain end and rotor blade, resulting in a decrease in the exerted torque.

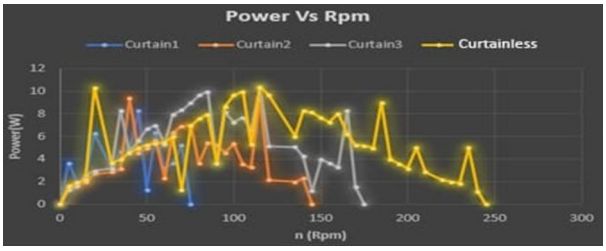

Fig. 7. Comparison of the Power vs RPM for elliptical rotor with different curtain types for β=45˚ and γ=15˚.

6.3 Flow physics analysis around the rotor

The Fig. 8 shows the fluid pressure, velocity, velocity stream line, velocity vector, eddy viscosity distributions are obtained from numerical analysis for modified savonius rotor with curtain at rotor position of 45˚ rotor angle. The maximum fluid pressure of 53.56 Pa, velocity of 21.75 m/s, velocity stream line of 22.43 m/s, velocity vector of 22.42 m/s and eddy viscosity of 0.068 Pa s are obtained. The Fig. 9 shows the fluid pressure, velocity, velocity stream line, velocity vector, eddy viscosity distributions are obtained from numerical analysis for modified savonius rotor without curtain at rotor position of 45˚ rotor angle. The maximum fluid pressure is 25.6 Pa, velocity of 16.42 m/s, velocity stream line of 16.93 m/s, velocity vector of 16.92 m/s and eddy viscosity of 0.04367 Pa s. The Fig. 10 shows the fluid pressure, velocity, velocity stream line, velocity vector, eddy viscosity distributions are obtained from numerical analysis for modified savonius rotor with curtain at rotor position of 60˚ rotor angle. The maximum fluid pressure is 89.48 Pa, velocity of 16.83 m/s, velocity stream line of 17.35 m/s, velocity vector of 17.35 m/s and eddy viscosity of 0.114 Pa-s. The Fig. 11 shows the fluid pressure, velocity, velocity stream line, velocity vector, eddy viscosity distributions are obtained from numerical analysis for modified savonius rotor without curtain at rotor position of 60˚ rotor angle. The maximum fluid pressure is 35.04 Pa, velocity of 15.82 m/s, velocity stream line of 12.13 m/s, velocity vector of 12.13 m/s and eddy viscosity of 0.01543 Pa s. The Fig. 12 shows the fluid pressure, velocity, velocity stream line, velocity vector, eddy viscosity distributions are obtained from numerical analysis for modified savonius rotor with curtain at rotor position of 90˚ rotor angle. The maximum fluid pressure is 64.91 Pa, velocity of 32.61 m/s, velocity stream line of 33.63 m/s, velocity vector of 33.63 m/s and eddy viscosity of 0.225 Pa-s. The Fig. 13 shows the fluid pressure, velocity, velocity stream line, velocity vector, eddy viscosity distributions are obtained from numerical analysis for modified savonius rotor without curtain at rotor position of 90˚ rotor angle. The maximum fluid pressure is 34.73 Pa, velocity of 17.96 m/s, velocity stream line of 15.55 m/s, velocity vector of 15.55 m/s and eddy viscosity of 0.07 Pa-s. These flow physics magnitudes changes with different values of fluid properties, which occurs due to angular deformation of fluid particles.

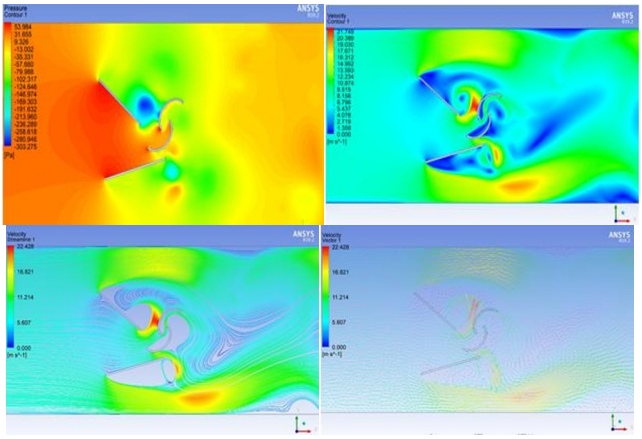

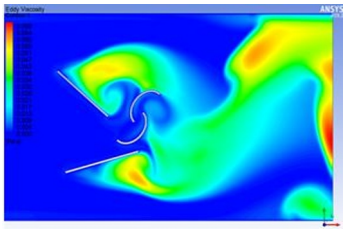

Fig. 8. The contour plots of (a) pressure distribution (b) velocity distribution (c) stream Line pattern (d) vector profile, (e) eddy viscosity generation at rotor position of 45° with curtain.

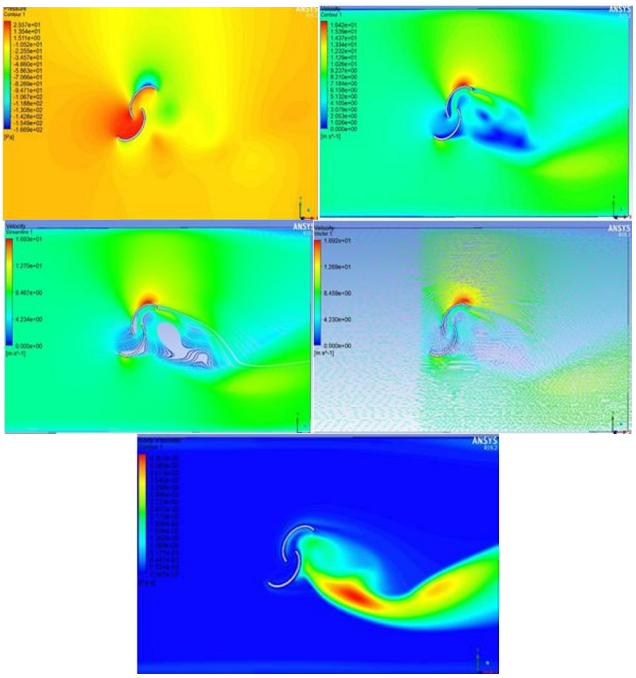

Fig. 9. The contour plots of (a) pressure distribution (b) velocity distribution (c) stream line pattern (d) vector profile, (e) eddy viscosity generation at rotor position of 45° without curtain.

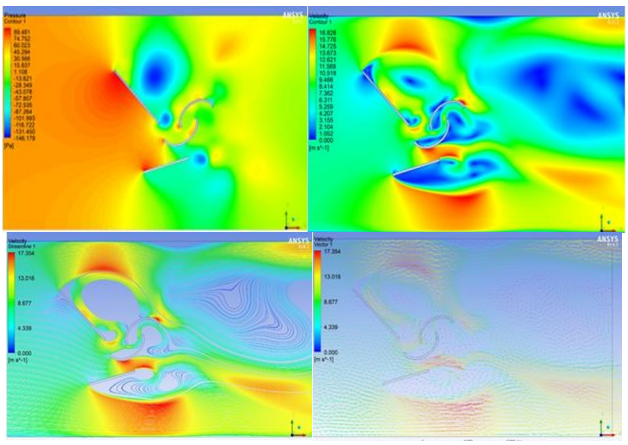

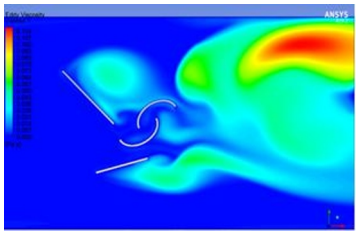

Fig. 10. The contour plots of (a) pressure distribution (b) velocity distribution (c) stream Line pattern (d) vector profile, (e) eddy viscosity generation at rotor position of 60° with curtain.

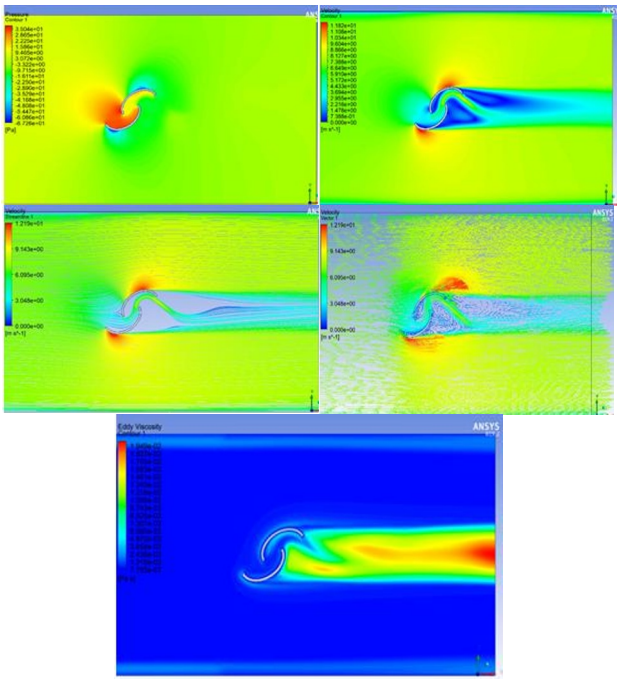

Fig. 11. The contour plots of (a) pressure distribution (b) velocity distribution (c) stream Line pattern (d) vector profile, (e) eddy viscosity generation at rotor position of 60° without curtain.

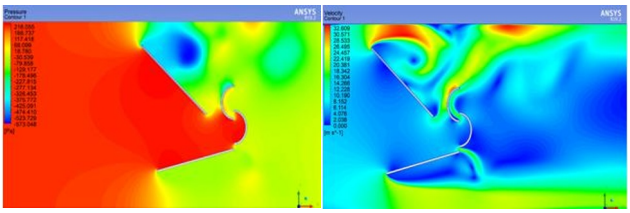

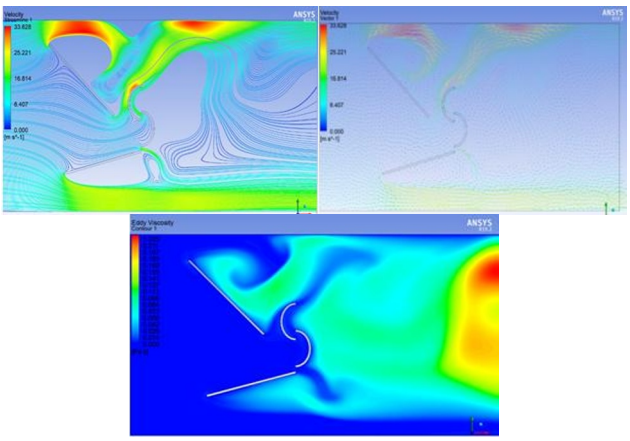

Fig. 12. The contour plots of (a) pressure distribution (b) velocity distribution (c) stream Line pattern (d) vector profile, (e) eddy viscosity generation at rotor position of 90° with curtain.

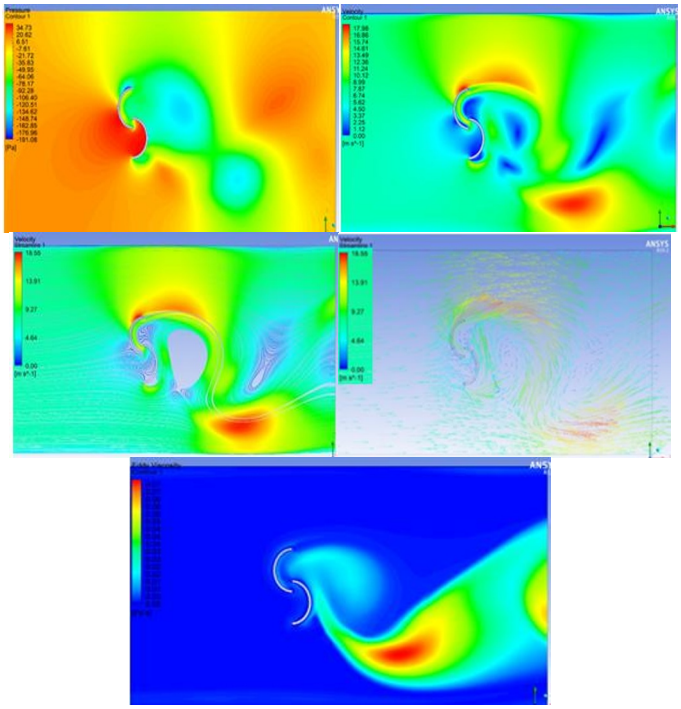

Fig. 13. The contour plots of (a) pressure distribution (b) velocity distribution (c) stream line pattern (d) vector profile, (e) eddy viscosity generation at rotor position of 90° without curtain.

7 Conclusions

The elliptical blade rotor has higher performance in comparison to conventional semi-circular profiles. A curtain, serving as a basic wind deflector, has been devised and

positioned in front of the rotor to safeguard the convex surface from the adverse impact of negative torque. The use of the curtain will also lead to an increase in the upstream wind velocity. The goal is to improve the efficiency of the Savonius wind turbine. The curtain has the ability to block the wind flow from reaching the convex blade, thereby enhancing the positive torque generated by the rotor. The numerical analysis indicates that the rotor with a curtain can outperform the rotor without a curtain when both are static at the same rotor positions. The following conclusions are drawn from the simulation:

- The rotor with curtain has achieved the highest torque values with curtain 1, the longest one.
- The best performance are obtained from γ=15˚ and β=45˚ has been obtained from curtain 1.
- When rotor position is 45˚ for elliptical rotor blades, the peak power magnitude of 10 W and the peak power magnitude of 8 W are obtained from conventional S-rotor.

Acknowledgment

The authors acknowledge the full support of Mechanical Engineering Department, National Institute of Technology Agartala, Tripura for providing wind tunnel and computer facility to conduct this research.

References

1. Aldoss, T. K., Kotb, M. A., "Theoretical calculations of the flow field around a Savonius rotor", *Wind Engineering,* **12**(3), pp.194-203, (1988).
2. Alom, N., Saha, U. K., "Performance Evaluation of Vent-augmented Elliptical-bladed Savonius Rotors by Numerical Simulation and Wind Tunnel Experiments", *Energy*, Vol. **152**, pp. 277-292, (2018).
3. Debnath, P., Gandhirajan, V., "A comprehensive review on design and development analysis and blade material selection of helical Savonius rotor", *Wind Engineering*, pp. 1-12, (2023).
4. Savonius, S. J., "The S-rotor and its applications", *Mech Eng,* **53**(5), pp. 333-8, (1931).
5. Menet, J. L., "A double-step Savonius rotor for local production of electricity: a design study", *Renewable Energy,* **29**, pp. 1843-62, (2004).
6. Percival, M. C., Leung, P. S., Datta, PK., "The development of a vertical turbine for domestic electricity generation", *Eur Wind Energy Conf Exhib,* (2014).
7. Altan, B. D., "Performance investigation of Savonius wind rotor with curtaining method", PhD thesis in mechanical engineering. Denizli, Turkey: Graduate School of Natural and Applied Sciences, Pamukkale University, p.147,(2006).
8. Altan, B. D., Atilgan, M., "An experimental and numerical study on the improvement of the performance of Savonius wind rotor, *Energy Conversion and Management,* Vol. **49**, pp. 3425-3432, (2008).
9. Altan, B. D., Atilgan, M., "An experimental study on improvement of a Savonius rotor performance with curtaining", *Experimental Thermal and Fluid Science*, Vol. **32**, pp. 1673-1678, (2008).
10. Altan, B. D., Atılgan, M., "The use of a curtain design to increase the performance level of a Savonius wind rotors", *Renewable Energy,* Vol. **35**, pp. 821-829, (2010).

11. Altan B. D., Atılgan M., "A study on increasing the performance of Savonius wind rotors", *Journal of Mechanical Science and Technology,* Vol. **26** (5), pp. 1493-1499, (2012).
12. Bhaumik, T., Gupta, R., "Performance measurement of a two bladed helical Savonius rotor", 37th National and 4th International Conference on Fluid Mechanics and Fluid power, (FMFP), Indian Institute of Technology, Madras, December 16-18, (2010).
13. Altan, B. D., Atilgan, M., "The use of a curtain design to increase the performance level of a Savonius wind rotors", *Renewable Energy*, Vol. **35**, pp. 821-829, (2010).
14. Kamoji, M. A., Kedare, S. B., Prabhu, S. V., "Experimental investigations on single stage modified Savonius rotor", *Applied Energy,*Vol. **86**, Issues 7-8, July-August 2009, pp. 1064-1073, (2009).
15. Mohamed, M. H., Janiga, G., Pap, E., Thévenin D., "Optimization of Savonius turbines using an obstacle shielding the returning blade", *Renewable Energy,* Vol. **35**, pp. 2618-2626, (2010).
16. Debnath, P., Gupta, R., Pandey, K. M., "Performance Analysis of the Helical Savonius Rotor Using Computational Fluid Dynamics", *ISESCO Journal of Science and Technology,* Vol.**10** (18), pp.17-28, (2014).
17. Le, A. D., Duc, B. M., Hoang, T. V., Tran, H. T., "Modified Savonius Wind Turbine for Wind Energy Harvesting in Urban Environments", *Journal of Fluids Engineering,* Vol. **144** / 081501-1, (2022).
18. Alom N., "Influence of curtain plates on the aerodynamic performance of an elliptical bladed Savonius rotor (S-rotor)", *Energy Systems,* Vol. **13**, pp. 265-280, (2022).
19. Ramarajan, J., Jayavel, S., "Performance Improvement in Savonius Wind Turbine by Modification of Blade Shape",*Journal of Applied Fluid Mechanics,* Vol. **15**, No. 1, pp. 99-107, (2022).
20. Kacprzak, K., Liskiewicz, G., Sobczak, K., "Numerical investigation of conventional and modified Savonius wind Turbines", *Renewable Energy*, Vol. **60**, pp. 578-585, (2013).
21. Tartuferi, M., D'Alessandro, V., Montelpare, S., Ricci, R., "Enhancement of Savonius wind rotor aerodynamic performance: a computational study of new blade shapes and curtain systems", *Energy,* Vol. **79**, pp. 371-384, (2015).